

Photoinduced helical inversion in cholesteric liquid crystal cells with homeotropic anchoring

Igor Gvozдовskyy,^{1,4} Oleg Yaroshchuk,^{1,*} Marina Serbina,² and Rumiko Yamaguchi³

¹*Institute of Physics of the National Academy of Sciences of Ukraine, Prospekt Nauki, 46, 03680 Kyiv, Ukraine*

²*Institute for Scintillation Materials of STC "Institute for Single Crystals" of the National Academy of Sciences of Ukraine, Lenin Ave., 60, 61001 Kharkiv, Ukraine*

³*Akita University, Department of Electrical and Electronic Engineering, 1-1 Tegatagakuen-cho, Akita 010, Japan*

⁴igvozdz@gmail.com

^{*}o.yaroshchuk@gmail.com

Abstract: Structural changes caused by the optically induced helical inversion in the cholesteric liquid crystal cells with homeotropic anchoring are studied. In a one-step exposure, a sequence of structural transformations "lying left-handed helix – unwound homeotropic state – lying right-handed helix" is realized. In this process, smooth expansion of a left-handed helix, transition to an unwound state, emergence and smooth compression of a right-handed helix was observed. The unwound state was maintained over a rather wide range of exposures. Well-oriented and highly periodic fingerprint textures capable of the above mentioned structural changes were obtained by rubbing the aligning substrates. This allowed for obtaining photo-tunable diffraction gratings and using them to demonstrate new beam steering principle. Also, pitch reversal suggested new options for optical recording, in particular contrast reversal and edge enhancement.

© 2012 Optical Society of America

OCIS codes: (230.3720) Liquid-crystal devices, (230.1950) Diffraction gratings, (210.4810) Optical storage-recording materials.

References and links

1. P. G. de Gennes and J. Prost, *The Physics of Liquid Crystals* (Oxford University Press, 1993).
2. P. Oswald and P. Pieranski, *Nematic and Cholesteric Liquid Crystals: Concept and Physical Properties Illustrated by Experiments* (CRC Press, 2005).
3. D. Demus and L. Ritcher, *Textures of Liquid Crystals* (Wiley VCH, 1980).
4. T. K. Gaylord and M. G. Moharam, "Thin and thick gratings: terminology clarification," *Appl. Opt.* **20**(19), 3271–3273 (1981).
5. D.-K. Yang, J. W. Doane, Z. Yaniv, and J. Glasser, "Cholesteric reflective display: drive scheme and contrast," *Appl. Phys. Lett.* **64**(15), 1905–1907 (1994).
6. B. Taheri, J. W. Doane, D. Davis, and D. St. John, "Optical properties of bistable cholesteric reflective displays," *SID Int. Symp. Digest Tech. Papers* **27**, 39–42 (1996).
7. Z. Li, P. Desai, R. B. Akins, G. Ventouris, and D. Voloschenko, "Electrically tunable color for full-color reflective displays," in *Liquid Crystal Materials, Devices, and Applications VIII*, L.-C. Chien, ed., *Proc. SPIE* **4658**, 7–13 (2002).
8. D. J. Broer, J. Lub, and G. N. Mol, "Wide-band reflective polarizers from cholesteric polymer networks with a pitch gradient," *Nature* **378**(6556), 467–469 (1995).
9. L. Li, J. Li, B. Fan, Y. Jiang, and S. M. Faris, "Reflective cholesteric liquid crystal polarizers and their applications," *Proc. SPIE-Int. Soc. Opt. Eng.* **3560**, 33–40 (1998).
10. Y.-C. Hsiao, C.-Y. Tang, and W. Lee, "Fast-switching bistable cholesteric intensity modulator," *Opt. Express* **19**(10), 9744–9749 (2011).
11. I. P. Ilchishin, E. A. Tikhonov, V. G. Tishchenko, and M. T. Shpak, "Generation of a tunable radiation by impurity cholesteric liquid crystals," *JETP Lett.* **32**, 27–30 (1980).
12. C. Denekamp and B. L. Feringa, "Optically active diarylethenes for multimode photoswitching between liquid crystalline phases," *Adv. Mater. (Deerfield Beach Fla.)* **10**(14), 1080–1082 (1998).
13. S. Kurihara, S. Nomiyama, and T. Nonaka, "Photochemical control of the macrostructure of cholesteric liquid crystals by means of photoisomerization of chiral azobenzene molecules," *Chem. Mater.* **13**(6), 1992–1997 (2001).

14. M. Brehm, H. Finkelmann, and H. Stegemeyer, "Orientation of cholesteric mesophases on lecithin-treated surfaces," *Ber. Bunsenges. Phys. Chem* **78**, 883–886 (1974).
15. D. Subacius, P. J. Bos, and O. D. Lavrentovich, "Switchable diffractive cholesteric gratings," *Appl. Phys. Lett.* **71**(10), 1350–1352 (1997).
16. P. Oswald, J. Baudry, and S. Pirkel, "Static and dynamic properties of cholesteric fingers in electric field," *Phys. Rep.* **337**(1-2), 67–96 (2000).
17. S. V. Shiyankovskii, D. Voloshchenko, T. Ichikawa, and O. D. Lavrentovich, "Director structures of cholesteric diffraction gratings," *Mol. Cryst. Liq. Cryst. (Phila. Pa.)* **358**(1), 225–236 (2001).
18. A. Y.-G. Fuh, Ch.-H. Lin, and Ch.-Y. Huang, "Dynamic pattern formation and beam-steering characteristics of cholesteric gratings," *Jpn. J. Appl. Phys.* **41**(Part 1, No. 1), 211–218 (2002).
19. J.-J. Wu, F.-C. Chen, Y.-S. Wu, and S.-H. Chen, "Phase gratings in pretilted homeotropic cholesteric liquid crystal films," *Jpn. J. Appl. Phys.* **41**(Part 1, No. 10), 6108–6109 (2002).
20. I. Smalukh, B. Senyuk, P. Palfy-Muhoray, O. D. Lavrentovich, H. Huang, E. Gartland, V. Bodnar, T. Kosa, and B. Taheri, "Electric-field-induced nematic-cholesteric transition and three-dimensional director structures in homeotropic cells," *Phys. Rev. E Stat. Nonlin. Soft Matter Phys.* **72**, 0617071–06170716 (2005).
21. In addition to this effect, the short-pitch helical structures ($p = 0.3\text{--}0.6\ \mu\text{m}$), known as uniform lying helix (ULH), can also be switched due to the flexoelectric effect. In this case, the applied electric field causes fast rotation of cholesteric helix in the cell plane due to the linear coupling between an electric polarization and splay/bend deformations of LC. The ULH texture can be transformed to the fingerprint texture in the electric field at values close to the unwinding voltage. In the present studies we are limited to the long-pitch CLC, which exhibit clear fingerprint textures at a zero field.
22. P. E. Cladis and M. Kleman, "The cholesteric domain structure," *Mol. Cryst. Liq. Cryst. (Phila. Pa.)* **16**(1-2), 1–20 (1972).
23. B. Y. Zeldovich and N. V. Tabiryán, "Equilibrium structure of a cholesteric with homeotropic orientation on the walls," *Sov. Phys. JETP* **56**, 563–566 (1982).
24. N. Tamaoki, "Cholesteric liquid crystals for color information technology," *Adv. Mater. (Deerfield Beach Fla.)* **13**(15), 1135–1147 (2001).
25. P. Witte, M. Brehmer, and J. Lub, "LCD components obtained by patterning of chiral nematic polymer layers," *J. Mater. Chem.* **9**(9), 2087–2094 (1999).
26. N. Venkataraman, G. Magyar, M. Lightfoot, E. Montbach, A. Khan, T. Schneider, J. W. Doane, L. Green, and Q. Lee, "Thin flexible photosensitive cholesteric displays," *J. Soc. Inf. Disp.* **17**, 869–873 (2009).
27. V. Vinogradov, A. Khizhnyak, L. Kutulya, Y. Reznikov, and V. Reshetnyak, "Photoinduced change of cholesteric LC pitch," *Mol. Cryst. Liq. Cryst. (Phila. Pa.)* **192**, 273–278 (1990).
28. B. L. Feringa, N. P. M. Huck, and A. M. Schoevaars, "Chiroptical molecular switches," *Adv. Mater. (Deerfield Beach Fla.)* **8**(8), 681–684 (1996).
29. P. Witte, J. C. Galan, and J. Lub, "Modification of the pitch of chiral nematic liquid crystals by means of photoisomerization of chiral dopants," *Liq. Cryst.* **24**(6), 819–827 (1998).
30. T. J. White, R. L. Bricker, L. V. Natarajan, V. P. Tondiglia, L. Green, Q. Li, and T. J. Bunning, "Electrically switchable, photoaddressable cholesteric liquid crystal reflectors," *Opt. Express* **18**(1), 173–178 (2010).
31. J. Ma, Ya. Li, T. White, A. Urbas, and Q. Li, "Light-driven nanoscale chiral molecular switch: reversible dynamic full range color phototuning," *Chem. Commun. (Camb.)* **46**(20), 3463–3465 (2010).
32. M. Mathews, R. S. Zola, S. Hurley, D. K. Yang, T. J. White, T. J. Bunning, and Q. Li, "Light-driven reversible handedness inversion in self-organized helical superstructures," *J. Am. Chem. Soc.* **132**(51), 18361–18366 (2010).
33. M. Mathews, R. Zola, D. Yang, and Q. Li, "Thermally, photochemically and electrically switchable reflection colors from self-organized chiral bend-core liquid crystals," *J. Mater. Chem.* **21**(7), 2098–2103 (2011).
34. Yu. Reznikov and T. Sergan, "Orientational transitions in a cell with twisted nematic liquid crystal," *Mol. Cryst. Liq. Cryst. (Phila. Pa.)* **330**(1), 375–381 (1999).
35. S. N. Yarmolenko, L. A. Kutulya, V. V. Vaschenko, and L. V. Chepeleva, "Photosensitive chiral dopants with high twisting power," *Liq. Cryst.* **16**(5), 877–882 (1994).
36. P. R. Gerber, "On the determination of the cholesteric screw sense by the Grandjean-Cano-method," *Z. Naturforsch. C* **35a**, 619–622 (1980).
37. S. V. Lagerwall, *Ferroelectric and Antiferroelectric Liquid Crystals* (Wiley-VCH, 1999).
38. H. Sato, H. Fujikake, Y. Iino, M. Kawakita, and H. Kikuchi, "Flexible grayscale ferroelectric liquid crystal device containing polymer walls and networks," *Jpn. J. Appl. Phys.* **41**(Part 1, No. 8), 5302–5306 (2002).

1. Introduction

Most practically used cholesteric liquid crystals (CLCs) are prepared on the basis of nematic liquid crystal (LC) mixtures doped with chiral additives, which induce a helical structure. They are called induced CLCs [1,2]. Depending on the nature of chiral dopant (ChD) and its interaction with the molecules of the nematic host, the cholesteric helix can be right- or left-handed. Like nematic LCs, cholesteric liquid crystals can form planar or homeotropic textures owing to different anchoring conditions at the aligning surfaces [1–3].

In the *planar texture* of the CLCs, the helical axis is perpendicular to the surface of the LC cell, and the phenomenon of selective light reflection (Bragg diffraction regime [4]) is observed with a maximum wavelength $\lambda_{\max} = np$, where n and p are the average refractivity index and the pitch of cholesteric helix, respectively. The helical pitch p is sensitive to temperature changes and external fields, which is the basis for various practical applications of CLCs (displays, thermal sensors, adjustable color filters and reflective polarizers, voltage-controlled light attenuating films, mirrorless lasers, *etc.*) [5–11].

The *homeotropic texture* of the CLCs, also known as fingerprint texture, is observed when the helical axis is parallel to the plane of LC cell. It should be noted that despite the fact that this texture is commonly associated with a pronounced homeotropic anchoring, it is frequently observed on the substrates not subjected to any alignment treatment, which seem to provide a weak homeotropic or even planar anchoring [12,13]. The spatial period and uniformity of these textures can be controlled by varying cell thickness d , pitch p , elastic constants of LC, anchoring coefficients, *etc* [14–20]. With a successful combination of these parameters and appropriate alignment treatment, highly uniform structures with regular and well-oriented patterns (fingers) can be formed. If the cell is subjected to external electric or magnetic field, a structural transition from the fingerprint to homeotropic or planar texture of a nematic LC can occur due to the coupling of the electric/magnetic field to the dielectric/magnetic anisotropy of LC [21]. In turn, the field action on the cells with planar anchoring may result in the transition from planar to fingerprint texture [15,17,20]. In case of well-oriented patterns this structure acts as a switchable diffraction grating (Raman-Nath diffraction regime [4]). The advantage of such gratings, as compared with other types of LC gratings, is the ability to quickly change the grating period. This, in turn, makes it possible to realize steering of light beams [15,18].

It has been shown that the lying cholesteric helix can be distorted or even completely suppressed when CLC is confined in a LC cell with sufficiently strong homeotropic anchoring [16,22]. There is a certain minimal helical pitch value:

$$p_{th} = 2d \frac{K_{22}}{K_{33}} \quad (1)$$

(K_{22} and K_{33} are elastic constants for twist and bend deformations, respectively), which can be achieved in a given cell [23]. If p is smaller than this threshold pitch p_{th} , the chiral torque is strong enough with respect to the elastic torque determined by orientational elasticity and anchoring, and twisted cholesteric structure can be observed. When $p > p_{th}$, the chiral torque is too weak and the system is not able to twist. In this case, homeotropic structure of nematic LC is observed.

Besides temperature variation and application of electric or magnetic fields, the cholesteric helix can also be efficiently controlled by light. The optical controlling offers several advantages, such as quick and smooth variation of structures and ease of patterning. Since initial and photoinduced structures have distinct optical properties, the photoaddressable CLCs are highly significant for optical recording systems, all-optical displays, photoadjustable light reflectors, *etc.* These devices do not require patterned conductive coatings (electrodes) and attached electronics that substantially reduces costs comparing with electronically driven counterparts. Besides, the resolution of these devices is rather high; it is limited only by the domain size of the cholesteric phase ($\sim 1\text{--}2 \mu\text{m}$) [24–26].

The main attention was previously paid to the planar textures, where a phototunable selective reflection could be realized [24–33]. This effect occurs due to the photoinduced change in conformation of ChD or LC host that affects twisting tension and, eventually, helical pitch in CLC.

In one of the few works related to photoinduced effects in the homeotropic texture, a transition from the fingerprint cholesteric to the nematic texture was observed [34]. In this

work, the authors used an induced CLC based on nematic LC 4-cyano-4'-pentylbiphenyl (5CB) and ChD 2-(4'-phenylbenzylidene)-*p*-menthane-3-one (PBM). UV irradiation caused *trans-cis* isomerization of PBM molecules [35], which resulted in a substantial decrease in their helical twisting power (HTP). When the pitch p exceeded the threshold value p_{th} , helix was completely suppressed and instead the nematic homeotropic texture was observed.

The aim of this work was to extend a sequence of photo-induced structural transitions in the CLC cells with homeotropic anchoring. This is achieved through the implementation of the cholesteric helix inversion, which was earlier attained in the cells with planar alignment [28,29,31,32] as well as in the non-aligned samples [13]. In this way, the photo-induced unwinding of lying cholesteric helix is completed by the transition from the unwound (nematic) structure to the lying cholesteric helix with the opposite sense. By proper alignment treatment of homeotropically aligning substrates, well aligned fingerprint textures (diffraction gratings in optical sense) that undergo structural transformations mentioned above are obtained. We demonstrate that these results give additional options for optical recording in CLC and suggest a new beam steering principle.

2. Idea and experimental details

In the literature, several methods of inversion of the cholesteric helix are described. In [28,31,32] the inversion is realized by using single ChD. Photo-excitation of these molecules leads to their conversion to another isomeric form, characterized by the chirality of the opposite sense.

In contrast, we used the two-dopant approach similar to that described in papers [25,29]. With this approach, the cholesteric mixture contains two CDs of opposite chiralities so that the resulting helix is left- or right-handed, depending on relative concentration of the dopants. One of these dopants is photosensitive, while the other one is insensitive to the light that causes excitation of the first dopant. In the initial state, the concentrations of these dopants are chosen so that the twisting direction is determined by the photosensitive ChD. The irradiation depletes the photosensitive ChD, resulting in weakening of the twisting tension caused by this dopant and unwinding of cholesteric helix. At a certain exposure dose, twisting tensions caused by the two dopants cancel each other and thus completely unwound (nematic) structure is observed. The following exposure results in further depletion of photosensitive ChD. The elastic torque caused by this dopant becomes weaker than the torque caused by the non-photosensitive dopant, which leads to twisting of LC in the direction opposite to the initial one. The new-formed helix strengthens with further irradiation.

To realize this scenario we used the right-handed ChD ZLI-3786 (R811) obtained from Merck and the left-handed ChD PBM synthesized at Institute for Single Crystals, NAS of Ukraine [35]. UV spectra of the dopants in hexane solution ($C = 10^{-4}$ mol/l) before and after UV irradiation are shown in Fig. 1.

In these measurements the solutions were placed in quartz cuvettes with a thickness $d = 1$ cm and irradiated with a full spectrum UV light, directly or through the glass plate. This plate was used as a filter cutting off the light with wavelengths shorter than 300 nm. As seen from Figs. 1(a) and 1(b), under full-spectrum UV irradiation, absorption band of each dopant decreases, *i.e.*, both dopants are involved in photoreactions. At the same time, when the short-wavelength range (UV radiation with $\lambda < 300$ nm) is cut off, only PBM dopant undergoes photoconversion (Figs. 1(c) and 1(d)). According to [35], this process is *trans-cis* isomerization, and HTP of *cis*-isomer is much lower than that of *trans*-isomers. Thus, when irradiated through a glass filter, the left-handed dopant PBM can be considered as a photoreactive, while the right-handed dopant R811 as a non-photoreactive one. The same is true for the CLC based on these dopants confined in the glass cells, because the glass substrates act as cut off filters for the shortwave UV light. This suggests that ChDs are correctly selected for using in glass LC cells.

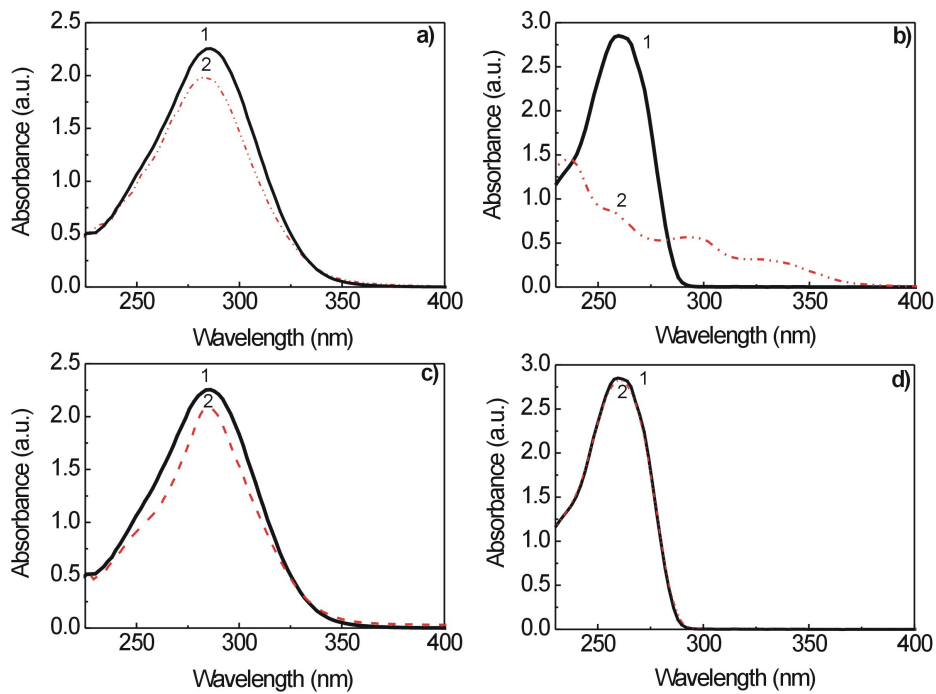


Fig. 1. Absorption spectra of PBM (a, c) and R811 (b, d) in hexane solution before and after UV irradiation. Spectra (a, b) correspond to direct irradiation, and (c, d) to irradiation through a glass plate. Numbers 1 and 2 stand for the spectra before and after 45 min irradiation, respectively.

The chiral dopants were dissolved in nematic LC MLC6884 (Merck) with negative dielectric anisotropy. The cholesteric mixture was prepared with concentrations $C_{PBM} = 1$ wt. % and $C_{R811} = 1.8$ wt. %. In addition, as reference samples, the corresponding single chiral dopant mixtures were prepared.

To obtain homeotropic alignment of CLC, we used polyimide SE1211 (Nissan, Japan). The polyimide films were deposited on glass substrates by spin-coating method (3000 rpm, 30 s), then annealed (180°C, 30 min) and, if necessary, unidirectionally rubbed. Using these substrates the cells with antiparallel rubbing directions were assembled with a cell thickness d set by mylar spacers and verified by the interference method. In studies of structural transformations under UV radiation d was 10, 16 and 20 μm , while in laser beam diffraction experiments it was fixed at 18 μm .

Additionally, to estimate the helical sense of the cholesteric mixtures for various exposure doses, wedge-like cells with planar anchoring conditions were prepared. The planar anchoring was provided by films of polyimide AL3046 (JSR, Japan), which were prepared by spin-coating method (3000 rpm, 30 s), annealed (190°C, 60 min) and unidirectionally rubbed. The thickness of wedge-like cells was about 20 μm . The helical sense was determined by Cano-Grandjean method as described in [36].

Illumination of LC cells was carried out by a high-pressure UV lamp UV-P 280 (Panacol, Germany). The integrated UV radiation intensity was 40 mW/cm^2 . The LC textures were observed by using a polarizing microscope Biolar (Poland) equipped with a digital camera Nikon D80 (Japan). The UV absorption spectra prior to UV irradiation and after fixed exposure doses were recorded in 230-450 nm range using a Hitachi 330 spectrophotometer.

Diffraction gratings based on fingerprint textures were characterized by studying diffraction of He-Ne laser beam traversing the LC cell. The intensities of the incident beam, I_0 , and the first-order diffraction beam, I_1 , were measured by photodetector and used to calculate the first order diffraction efficiency η according to formula $\eta = I_1/I_0$.

3. Results and discussion

Figure 2 shows the cell based on non-rubbed PI layers for homeotropic alignment, which is filled with the cholesteric mixture MLC6884/PBM/R811. The periphery part of this cell is a non-irradiated area showing the texture of the initial left-handed cholesteric LC. The three vertical strips are the areas subjected to different exposure doses. Area 1 irradiated for 5 s demonstrates cholesteric structure with a left-handed helix. Area 2 irradiated for 120 s corresponds to unwound (nematic) state. Finally, area 3 irradiated for 300 s corresponds to the right-handed helix. The sense of the cholesteric helix for each exposure dose was determined by using a wedge cell with planar anchoring.

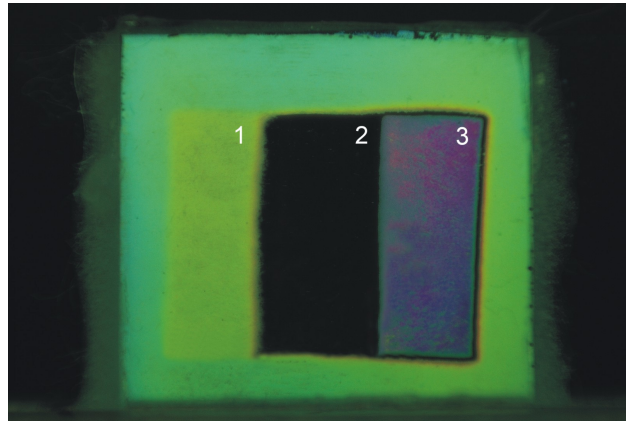


Fig. 2. Photograph of LC cell ($d=20\ \mu\text{m}$) with homeotropic anchoring filled with the cholesteric mixture MLC6884/PBM/R811. The cell is irradiated through a proximity mask with UV light so that the exposure time is 5, 120 and 300 s in areas 1, 2 and 3, respectively. These areas represent (1) a left-handed cholesteric LC, (2) nematic LC and (3) a right-handed cholesteric LC. The cell is viewed between two crossed polarizers.



Fig. 3. Microphotographs corresponding to areas 1, 2 and 3 in Fig. 2; (a) fingerprint texture of a left-handed cholesteric LC, (b) compensated nematic texture, and (c) fingerprint texture of a right-handed cholesteric LC.

The microscopic images corresponding to areas 1, 2 and 3 in Fig. 2 are presented in Fig. 3. In areas 1 and 3 the fingerprint textures are observed. These textures are not well aligned, because aligning layers in the cell are not rubbed. Some alignment in these areas is caused by directional filling of CLC in the cells. The period of the textures is equal to helical pitch. The

photo-switching from a left-handed to a right-handed helix occurs through the unwound state that is reasonable from topological point of view.

The helical pitch values, p , were determined from the fingerprint texture periods for different exposure times, τ_{exp} . The p vs. τ_{exp} plots for the single-dopant mixtures, MLC6884/PBM and MLC6884/R811, and two-dopant mixture MLC6884/PBM/R811 are shown in Fig. 4, case (a) and (b), respectively. For the MLC6884/R811 mixture, the pitch p is independent of the exposure time, while for the MLC6884/PBM mixture it monotonically grows with τ_{exp} (Fig. 4(a)). Thus, HTP of PBM is photocontrolled, while that of ChD R811 is insensitive to UV light. This further confirms that chiral dopants were chosen properly.

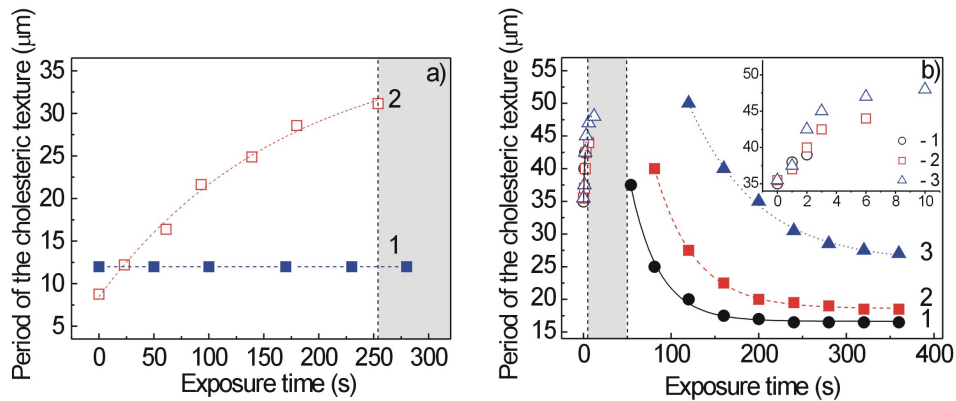


Fig. 4. The pitch length vs. exposure time curves. (a) Single-dopant cholesteric mixtures MLC6884/R811 (curve 1) and MLC6884/PBM (curve 2) in the cells with thickness $d = 16 \mu\text{m}$. (b) Two-dopant cholesteric mixture MLC6884/PBM/R811 in the cells with $d = 10, 16$ and $20 \mu\text{m}$, curves 1, 2, and 3, respectively. Open symbols correspond to left-handed helical structures, and solid symbols denote the right-handed helical structures. The areas highlighted in gray correspond to unwound cholesteric structure realized for the PBM containing mixtures in the cells with $d = 10 \mu\text{m}$. The inset depicts the ascending branches of $p(\tau_{exp})$ dependences in an enlarged scale.

For the two-dopant mixture MLC6884/PBM/R811 the $p(\tau_{exp})$ dependence consists of two branches shown in Fig. 4(b). The initial ascending branch (open symbols) corresponds to the left-handed helical structures, while the descending branch (solid symbols) is associated with the helical structures of the opposite sense. The branches of the $p(\tau_{exp})$ curve are separated with a distinct range of exposure time corresponding to doses for which the unwound state rather than helical state is realized.

As can be seen from Fig. 4(b), the pitch p of the two-dopant mixture is tuned in a rather wide range – from 35 to $50 \mu\text{m}$ (a left-handed helix) and from $50 \mu\text{m}$ to $17 \mu\text{m}$ (a right-handed helix), and this range depends on the cell thickness.

The observed behavior of $p(\tau_{exp})$ curves suggests that the structural transformations in the samples occur according to the scenario earlier conceived. The ascending branch of the $p(\tau_{exp})$ curve reflects the UV-induced unwinding of the initial left-handed helix. This is due to *trans-cis* photoisomerization of PBM leading to weakening of twisting tension caused by this dopant. The descending branch is associated with the helix of opposite sense caused by the R811 dopant. An important difference compared to the previously conceived scheme is that the transient unwound state is formed in a wide range of exposure doses, rather than at some fixed dose. This range of doses corresponds to the range of inaccessible values of pitch, $p > p_{th}$. In other words, the structures associated with weak twisting stress (large helical pitch), cannot be realized. We attribute this primarily to a strong homeotropic anchoring in our cells.

The situation is similar to the surface stabilized layers of ferroelectric LCs, in which strong anchoring suppresses helix of smectic C* phase [37].

As can be seen from Fig. 4(b), the $p(\tau_{exp})$ dependencies for the cells with different thicknesses are essentially different. For all scale of irradiation time, the helical structure period increases with the cell thickness d . In our opinion, the only feasible reason for such behavior is one-side irradiation. It is assumed that the *trans-cis* photoisomerization of PBM molecules occurs non-uniformly across the cells, because the light beam, passing through the LC, is attenuated. This effect becomes more pronounced with larger cell thickness. In order to verify our assumption, the gradient of light intensity across the cells was minimized by simultaneous irradiation of cells from two sides. In agreement with our assumption, the period of textures in the 16 μm and 20 μm cells after prolonged irradiation approached the period value as in a 10 μm cell. Extension of the range of exposure doses corresponding to unwound state and its shift to higher doses with a cell thickness, d , may also be attributed to non-uniformity of photoconversion of PBM molecules across the cells. As can be seen in Fig. 4(b), the threshold value of pitch p_{th} increases with the cell thickness d in agreement with the theoretically derived expression (1).



Fig. 5. The photoinduced inversion of optical images in CLC cell with homeotropic anchoring. The 10 μm cell based on non-rubbed SE1211 alignment layers and filled with CLC MLC6884/PBM/R811 is viewed between crossed polarizers (picture 1). At first the cell is irradiated during 40 s through a mask with the transparent areas in an “IOP” form (picture 2) and then during 40 s entirely (picture 3). As a result, image 3 is inverted to image 2.

The implemented sequence of cholesteric-nematic-cholesteric structural transitions suggests a unique principle for recording and processing of optical images in CLC cells, particularly interesting for all-optical displays. The distinctive feature of this process is the possibility of contrast reversal, when light areas become dark and vice versa. An example of this approach is demonstrated in Fig. 5. In this example, the cell based on non-rubbed alignment layers of PI SE1211 and filled with CLC MLC6884/PBM/R811 (picture 1) is irradiated through a mask with the transparent areas in the form of “IOP” letters. After a short exposure, the “IOP” letters switch to a compensated nematic phase and become black, contrasting well with the cholesteric texture (background in picture 2). In this picture, the edge enhancement is also observed, which is apparently due to partial unwinding of the left-handed helix on the border with the compensated nematic area. After further irradiation of the cell without a mask, in the background a left-handed cholesteric LC switches to the compensated nematic LC, while the compensated nematic in “IOP” shaped areas switches to a right-handed cholesteric LC. Due to intensive light scattering, these areas contrast with a dark background (picture 3). The latter image is negative to the former one, *i.e.*, through light irradiation the contrast reversal is attained.

It should be noted that along with the cells containing patterns of cholesteric and nematic textures, the cells with the patterns of left-handed and right-handed cholesteric textures can be obtained. However, the latter patterns are not stable enough due to diffusion of ChDs leading to mutual destruction of helices with the opposite sense. It seems possible to stabilize such structures with polymer networks and walls [38].

Subsequently, the series of structural transitions described above was implemented for oriented textures. To attain oriented fingerprint textures, the aligning layers were unidirectionally rubbed. At optimized rubbing conditions, well-oriented and highly periodic

textures were obtained. Figure 6(a) shows that these textures change, passing the steps previously observed for non-oriented textures.

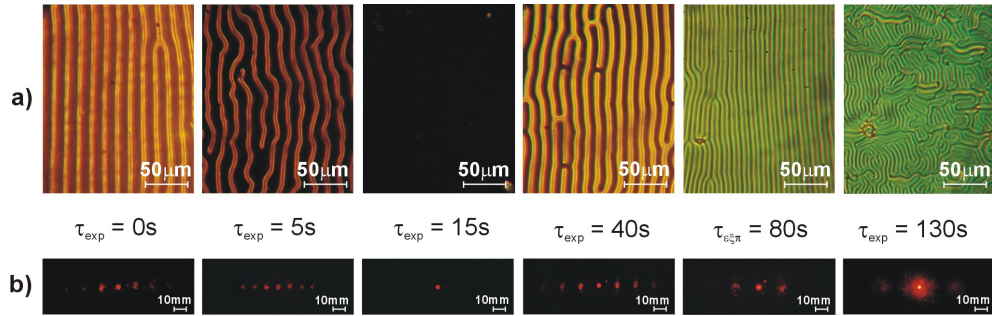


Fig. 6. (a) Microphotographs of aligned fingerprint textures (gratings) formed after different exposure times. Thickness of LC cell is $18\mu m$. Observation under crossed polarizers. (b) Diffraction patterns corresponding to gratings in Fig. 6(a).

The oriented fingerprint textures act as transmissive diffraction gratings with a period Λ equal to the cholesteric pitch p . The grating period change under irradiation (Fig. 6(a)) is accompanied with a nonmonotonic change of diffraction efficiency η and diffraction angle θ (Fig. 7). Unwinding of cholesteric helix, *i.e.*, the increase of Λ with τ_{exp} ($\tau_{exp} < 10$ s) is accompanied with increasing of diffraction efficiency η (solid squares) and decreasing of diffraction angle θ (open squares). The range $\tau_{exp} = 10$ -30 s corresponds to the compensated nematic state, where diffraction of light is not observed. The dependences shown in Fig. 7 by solid and open circles ($\tau_{exp} > 30$ s), reflect emergence of a right-handed cholesteric helix and its compression with exposure time.

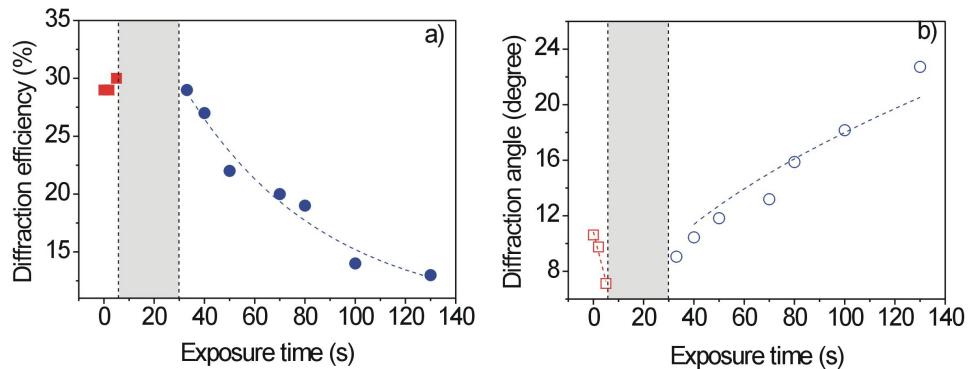


Fig. 7. Diffraction efficiency (a) and diffraction angle (b) as function of exposure time for periodic structure of CLC MLC6884/PBM/R811 in the $18\mu m$ cell with rubbed layers of homeotropic polyimide. In the plots, the area highlighted in gray corresponds to unwound cholesteric structure (absence of grating).

This process results in a wide-range controlling of diffraction efficiency ($\eta = 0$ -30%, Fig. 7(a)) and diffraction angle ($\theta = 9^\circ$ -23°, Fig. 7(b)). The latter result suggests a new principle of beam steering when the beam direction is controlled by light rather than heating or electric field [15,18]. Using samples with helical inversion, the beam can be deviated in one direction or successively in two opposite directions just in one-step exposure (Fig. 8).

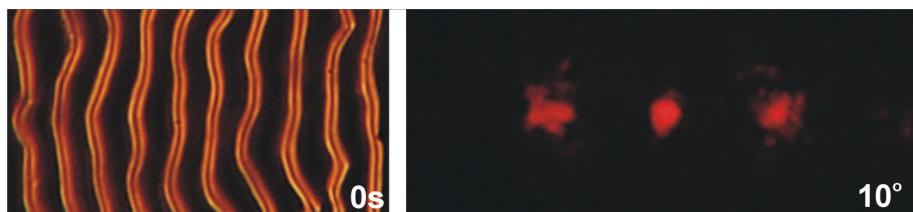


Fig. 8. Single-frame from a [Media 1](#) demonstrating new beam steering principle. The left picture shows changing of fingerprint grating and the right one shows a change in position of diffraction patterns with exposure time.

Of course, the practical implementation of the proposed principles is associated with improvement of periodic structures. Their heterogeneity, especially for small periods, increases losses and deformation of beams, primarily due to the scattering of light. This problem is particularly essential for $\tau_{exp} = 130$ s in Fig. 6. Further optimization of chiral dopants and their ratio in LC is also important. The weak point of the studied CLC mixtures is irreversible photoconversion of molecules of ChD. The use of ChDs with reversible photoconversion can allow us to attain reversible changes in the grating parameters, in particular, polycyclic changes in the efficiency and diffraction angle. For this purpose, chiral dopants providing a broad-range reversible variation of cholesteric pitch are especially promising. For planar CLC textures, such dopants have been recently tested in [31,32].

4. Conclusions

Thus, a light-induced inversion of helical sense accompanied with a smooth and broad-range variation of helical pitch and a sequence of photoinduced structural transitions “left-handed cholesteric LC - nematic LC - right-handed cholesteric LC” is realized in LC cells with homeotropic anchoring. As well as the cholesteric phases, the compensated nematic phase was stable and it was observed in a rather wide range of exposures. By a proper rubbing treatment of homeotropically aligning layers, well-aligned fingerprint textures undergoing the same sequence of structural transformations are obtained. Based on these results, optical controlling of CLC gratings is realized and used to develop a new beam steering principle. It is also demonstrated that pitch reversal provides additional opportunities for optical recording in CLC, such as contrast reversal and edge enhancement. One can expect that new features of the studied samples will be discovered at their electric addressing [26].

Acknowledgments

The authors thank Dr. W. Becker from Merck for providing LC MLC-6884 and chiral dopant R-811, Prof. L. Kutulya for kind provision of PBM material, and Prof. L. Lisetski for valuable discussions. O. Ya. acknowledges financial support from Japan Society for Promotion of Science under Grant No. L-10535.